




Article

A Satellite-Based High-Resolution (1-km) Ambient PM_{2.5} Database for India over Two Decades (2000–2019): Applications for Air Quality Management

Sagnik Dey ^{1,2,*} , Bhavesh Purohit ¹, Palak Balyan ¹, Kuldeep Dixit ¹ , Kunal Bali ¹, Alok Kumar ¹, Fahad Imam ¹, Sourangsu Chowdhury ³, Dilip Ganguly ¹ , Prashant Gargava ⁴ and V. K. Shukla ⁴

¹ Centre for Atmospheric Sciences, IIT Delhi, New Delhi 110000, India; ast182713@cas.iitd.ac.in (B.P.); Palak.Balyan@cas.iitd.ac.in (P.B.); kdixit@cas.iitd.ac.in (K.D.); Kunal.Bali@cas.iitd.ac.in (K.B.); ird12852@cas.iitd.ac.in (A.K.); ird12990@cas.iitd.ac.in (F.I.); dilipganguly@cas.iitd.ac.in (D.G.)

² Centre of Excellence for Research on Clean Air, IIT Delhi, New Delhi 110000, India

³ Max Planck Institute for Chemistry, 55128 Mainz, Germany; S.Chowdhury@mpic.de

⁴ Central Pollution Control Board, New Delhi 110000, India; prashant.cpcb@gov.in (P.G.); vkshukla.cpcb@nic.in (V.K.S.)

* Correspondence: sagnik@cas.iitd.ac.in; Tel.: +91-11-2659-1315

Received: 17 August 2020; Accepted: 9 October 2020; Published: 26 November 2020



Abstract: Fine particulate matter (PM_{2.5}) is a major criteria pollutant affecting the environment, health and climate. In India where ground-based measurements of PM_{2.5} is scarce, it is important to have a long-term database at a high spatial resolution for an efficient air quality management plan. Here we develop and present a high-resolution (1-km) ambient PM_{2.5} database spanning two decades (2000–2019) for India. We convert aerosol optical depth from Moderate Resolution Imaging Spectroradiometer (MODIS) retrieved by Multiangle Implementation of Atmospheric Correction (MAIAC) algorithm to surface PM_{2.5} using a dynamic scaling factor from Modern-Era Retrospective analysis for Research and Applications Version 2 (MERRA-2) data. The satellite-derived daily (24-h average) and annual PM_{2.5} show a R^2 of 0.8 and 0.97 and root mean square error of 25.7 and 7.2 $\mu\text{g}/\text{m}^3$, respectively against surface measurements from the Central Pollution Control Board India network. Population-weighted 20-year averaged PM_{2.5} over India is 57.3 $\mu\text{g}/\text{m}^3$ (5–95 percentile ranges: 16.8–86.9) with a larger increase observed in the present decade (2010–2019) than in the previous decade (2000 to 2009). Poor air quality across the urban–rural transect suggests that this is a regional scale problem, a fact that is often neglected. The database is freely disseminated through a web portal ‘satellite-based application for air quality monitoring and management at a national scale’ (SAANS) for air quality management, epidemiological research and mass awareness.

Keywords: PM_{2.5}; MAIAC; AOD; India; air quality

1. Introduction

Exposure to ambient fine particulate matter (PM_{2.5}) is one of the leading causes of health burden in India [1,2]. The rising ambient PM_{2.5} concentration [3,4] and its staggering health burden [5,6] led the Government of India to launch the National Clean Air Program (NCAP) in early 2018. Though the NCAP addressed air pollution as a national scale problem, its focus on the urban centres essentially fails to recognize the air quality status in the rural areas. This is reflected in the ground-based monitoring network maintained by the Central Pollution Control Board (CPCB) with all of the 230+ continuous and

650+ manual monitoring sites (www.cpcb.nic.in) deployed in the urban centres. Although the number of ground-based monitoring sites seems to be large, it is not adequate for air quality management [7] because (1) the network is disproportionately distributed (Figure A1 in the Appendix A); (2) PM_{2.5} monitoring started in 2009 (unlike PM₁₀ that has a longer record [8]), but the network expanded nationally only after 2015–2016; and (3) the manual monitoring sites only sample twice a week and do not provide continuous data. The population-weighted distance to the nearest monitoring site in India is estimated to be 80 km [7].

These limitations rendered the surface measurements inadequate for air quality management at a regional scale [9] and restricted the epidemiological community from using these data alone to generate indigenous evidence of air pollution health impacts consistently [10]. Furthermore, many cities in India do not have any surface measurements to determine if they are or are not non-attainment sites (with respect to the Indian annual national ambient air quality standard, NAAQS of 40 µg/m³). We earlier demonstrated the utility of satellite-derived aerosol products to infer surface PM_{2.5} and complement the surface measurements [3,5,11,12]. With the improvement of the spatial resolution of satellite-based aerosol optical depth (AOD) products and modelling techniques, we were able to track PM_{2.5} buildup in the Delhi national capital region (NCR) at a high resolution (1-km) over 15-years [13]. These analyses demonstrated the need to have a long-term PM_{2.5} national database for an efficient air quality management under the NCAP.

Broadly, there are two methods to estimate surface PM_{2.5} from satellite AOD. Several studies have adopted a regression-based or machine learning-based approaches that train the model with various geospatial variables [14,15]. In the other approach, a scaling factor (η , that is the ratio of PM_{2.5} and AOD) is derived to convert satellite AOD to PM_{2.5} [16–19]. The global database generated for the Global Burden of Disease (GBD) study derived the scaling factor from a chemical transport model at a coarse (usually 2° × 2.5°) resolution and interpolates it to match satellite AOD spatial resolution. Subsequently, the accuracy of the product was improved by fusion with the local surface measurements [20]. However, having a national database that is tuned against local surface measurements will be a better representative of the local conditions. Furthermore, the database can be updated as per the national requirement and used for policy.

In this work, we develop and present a satellite-based national PM_{2.5} database at a high resolution (1-km) for India over two decades (2000–2019). The database is used to understand the long-term trends in PM_{2.5}, the urban vs. rural air quality comparison, seasonal fluctuation in PM_{2.5} and the state-level statistics, all of which are highly important for air quality management.

2. Materials and Methods

2.1. Details of the Algorithm to Estimate PM_{2.5} from Satellite AOD

We build our algorithm based on the philosophy of the previous works following the scaling factor approach [3,16–19]. This scaling factor includes the impacts of local emissions, atmospheric processes, meteorology and regional transport on the AOD–PM_{2.5} relationship. Here, we derive η from the Modern-Era Retrospective analysis for Research and Applications (MERRA-2) reanalysis product because (1) MERRA-2 data are continuously available at near real-time, and (2) processing MERRA-2 data is computationally much less expansive than running a chemical transport model. We note that MERRA-2 spatial resolution is finer than that of the GEOS–Chem model that was utilized to derive η for the global data. We also analyze the Aerosol Robotic Network (AERONET) data to assess the satellite and MERRA-2 AOD products. The steps in the algorithm are as follows (Figure 1). To clarify the source of the various parameters discussed below, we denote the respective products from AERONET, satellite and reanalysis by using sub-scripts “AERO”, “sat” and “model”, respectively.

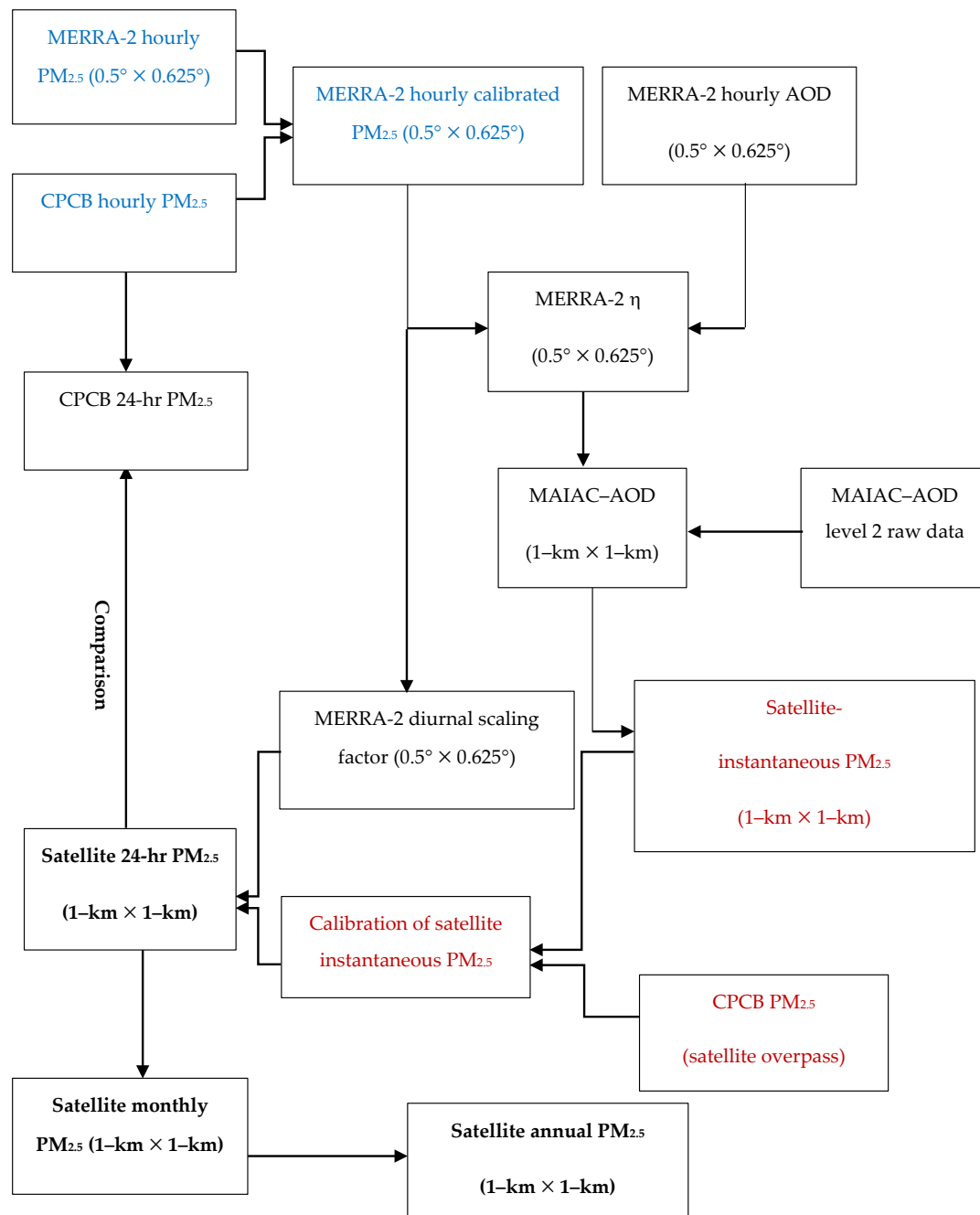


Figure 1. The flow chart of the entire process with the Modern-Era Retrospective analysis for Research and Applications Version 2 (MERRA-2) calibration steps shown in blue colored font, satellite fine particulate matter (PM_{2.5}) evaluation in red colored font and generation of the final products that are disseminated through the ‘satellite-based application for air quality monitoring and management at a national scale’ (SAANS) portal in bold black font.

First, we process level 2 AOD data retrieved by the Moderate Resolution Imaging Spectroradiometer (MODIS) using the Multiangle Implementation of Atmospheric Correction (MAIAC) algorithm at 1-km × 1-km resolution for each day (i) from 26 February 2000, to 31 December 2019. MAIAC provides global AOD retrievals over dark and bright surfaces using an explicit surface reflectance model and it features an improved cloud detection scheme, a general lack of bias in the urban areas and a better spatial coverage relative to the deep-blue or dark-target approach [21]. In this study, we have used the combined Terra and Aqua AOD product (MCD19A2) provided by the MODIS

science team. The combined product enhances the spatial and temporal coverage and provides a more representative AOD during 10:00 AM to 2:00 PM local time [21]. MAIAC AOD validation over South Asia revealed that it has a better accuracy than the deep blue and dark-target AOD products [22]. We also examine the product over India (Figure A2) and find that MODIS–MAIAC AOD at 550 nm shows a statistically significant ($p < 0.05$) correlation and root mean square error (RMSE) of 0.13 with AOD from AERONET [23] sites in India. MAIAC AOD is provided at 550 nm wavelength, therefore for a proper comparison, we estimate AERONET AOD at 550 nm wavelength from the spectral AOD measurements and Angstrom Exponent (α) at 440–870 nm wavelength following:

$$\text{AOD}_{550,\text{AERO}} = \text{AOD}_{500,\text{AERO}} \times \left(\frac{500}{550}\right)^{\alpha_{\text{AERO}}} \quad (1)$$

When the MAIAC–AOD tiles are merged, it shows a high variance along its swath edge. To minimize the edge effect across the swaths, we use the Savitzky–Golay filter [24] with a frame length of five pixels across the X- and Y-directions of the target pixel.

In the second step, we analyze aerosol products of MERRA-2 available at $0.5^\circ \times 0.625^\circ$ [25]. MERRA-2 $\text{PM}_{2.5}$ is estimated as:

$$\text{PM}_{2.5,\text{model}} = \text{Dust}_{2.5,\text{model}} + \text{SS}_{2.5,\text{model}} + \text{BC}_{\text{model}} + \text{OC}_{\text{model}} \times 1.6 + \text{SO}_4^{2-}{}_{\text{model}} \times 1.375 \quad (2)$$

where $\text{Dust}_{2.5,\text{model}}$ and $\text{SS}_{2.5,\text{model}}$ are dust and sea-salt masses in size bins smaller than $2.5 \mu\text{m}$, BC_{model} is black carbon, OC_{model} is organic carbon and $\text{SO}_4^{2-}{}_{\text{model}}$ is the sulfate. OC is multiplied by a factor of 1.6 to estimate total organic matter [26]. Sulfate in the MERRA-2 dataset is present in neutralized $(\text{NH}_4)_2\text{SO}_4$ form, so a factor of 1.375 is used [25]. MERRA-2 $\text{PM}_{2.5}$ is underestimated over the Indian region [27]. We therefore calibrate MERRA-2 hourly $\text{PM}_{2.5}$ with the coincident hourly $\text{PM}_{2.5}$ from 120 sites in the CPCB network that provide multi-year data from 2009 to 2019 (Figure A1). These CPCB stations use an automatic air quality monitoring system, where quality-control procedures are performed routinely to remove any unreliable, low-quality and invalid observations arising from instrument malfunction and electric power outage [28]. We note that the length of observations differs from site to site. To ensure enough samples, we use all quality-controlled data. We could not use the data from the manual monitoring sites because the robustness of the quality and the days when they are sampled are not consistent.

We train our calibration model for the 55 MERRA-2 grids having at least one CPCB site and develop a percentile-based calibration factor [3]. For every 10 percentile ranges, we estimate the ratio of surface $\text{PM}_{2.5}$ and MERRA-2-derived $\text{PM}_{2.5}$ for each site. Using the site-specific calibration factors representative for each month, we tune the MERRA-2 hourly $\text{PM}_{2.5}$ data in these grids close to the observed values and use the nearest neighbor algorithm to adjust the bias for the grids devoid of any CPCB site. Using this calibrated $\text{PM}_{2.5}$ and hourly AOD (at 550 nm) from MERRA-2, we estimate η for every day (i) and every grid (x and y) as:

$$\eta_{i,x,y,\text{model}} = \frac{\text{PM}_{2.5\ i,x,y,\text{model}}}{\text{AOD}_{i,x,y,\text{model}}} \quad (3)$$

We find that MERRA-2 and AERONET AOD show a statistically significant ($p < 0.05$ for $N = 4546$) R^2 of 0.71 (Figure A3) with a RMSE similar to that of MAIAC AOD. Therefore, we interpret that calibrating the MERRA-2 $\text{PM}_{2.5}$ is sufficient to improve the calibration of η and apply on satellite AOD.

In the third step, we interpolate η to finer resolution using spline interpolation to match the resolution of the AOD product ($1\text{-km} \times 1\text{-km}$). The spatial patterns of interpolated η for every month are shown in Figure A4. Wherever η values are high (>160), most of the particles within the column stay close to the surface, resulting in high $\text{PM}_{2.5}$ due to a stable boundary layer (e.g., winter months). Whenever the atmospheric condition is conducive for dispersion (e.g., in summer months), particles are raised above the boundary layer and hence although $\text{PM}_{2.5}$ remains moderate (between 100 to 160),

AOD remains high (i.e., moderate η values). During the monsoon, both AOD and $PM_{2.5}$ remain low and the high convective strength does not contain particles closer to the surface. As a result, η is found to be low (<100). We convert MAIAC AOD for the day i during the satellite overpass time (h) to $PM_{2.5}$ at the same resolution using the η values from Equation (2) as:

$$PM_{2.5,i,x,y,h,sat} = \eta_{i,x,y,model} \times AOD_{i,x,y,h,sat} \quad (4)$$

We call this $PM_{2.5}$ as the instantaneous $PM_{2.5}$ because the satellites carrying the MODIS sensor cross the Indian region between 10:00 AM and 2:00 PM local time, and therefore, the satellite-derived $PM_{2.5}$ does not represent the 24-h cycle.

We assume that the spatial heterogeneity in $PM_{2.5}$ within a coarse MERRA-2 grid (used to derive η) can be captured by the MAIAC AOD data at 1-km resolution and will not be affected much by the interpolation of η . We compare (Figure 2) the interpolated η from MERRA-2 with that derived directly for the grids having at least one CPCB site by taking the ratio of $PM_{2.5}$ (measured from the ground) and AOD (from MAIAC). Though most of the data points lie within 1:2 and 2:1 lines, the MERRA-2 η shows slightly low bias with respect to the in-situ data with a correlation coefficient that is statistically significant ($p < 0.05$) and a RMSE of 66.8 (that corresponds to an error of $20 \mu g m^{-3}$ in retrieved $PM_{2.5}$ for an AOD of 0.3). To minimize this bias in satellite-derived instantaneous $PM_{2.5}$ due to the interpolation of η to a finer resolution, in the fourth step, we perform the second calibration. We estimate the calibration factors for each 10 percentile ranges as the ratio of $PM_{2.5}$ measured at the surface during the satellite overpass time and satellite-derived instantaneous $PM_{2.5}$. Using the site-specific calibration factors representative for each month, we tune the satellite-derived instantaneous $PM_{2.5}$ data in these grids closer to the observed values and use the nearest neighbor algorithm to adjust the bias for the grids devoid of any CPCB site.

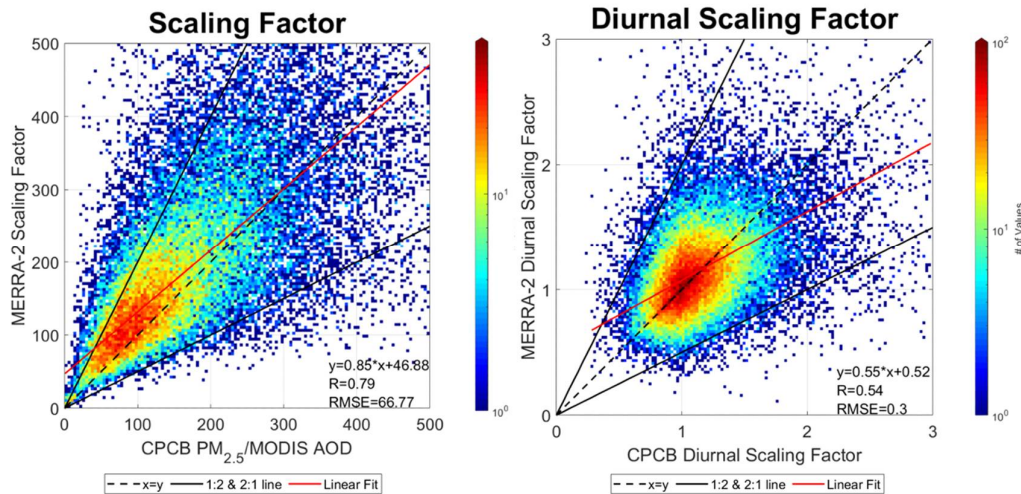


Figure 2. Regression statistics of the (left) scaling factor (η) and (right) diurnal scaling factor from MERRA-2 and ground-based measurements over India.

In the fifth step, we estimate the diurnal scaling factor (DSF) of each grid (x, y) for the conversion of calibrated satellite-derived $PM_{2.5}$ during the satellite overpass time (h) to the 24-h average of each day (i) using MERRA-2 data as:

$$DSF_{i,x,y,h,model} = \frac{PM_{2.5,i,x,y,24-h,model}}{PM_{2.5,i,x,y,h,model}} \quad (5)$$

The spatial patterns of the mean monthly diurnal scaling factors are shown in Figure A5. We find that the $PM_{2.5}$ concentrations during the satellite overpass time are lower than the 24-h average (hence

the ratio is >1) almost everywhere in every month, except over the Western Ghats during July and August and parts of Central India in May. We also compare the diurnal scaling factor derived from MERRA-2 with that from CPCB data (Figure 2). We find that the MERRA-2 diurnal scaling factor shows a statistically significant ($p < 0.05$) correlation with CPCB diurnal scaling factor, but with a low bias and a RMSE of 0.3. It implies that the retrieved 24-h $PM_{2.5}$ concentration is likely to be underestimated (as compared to the reference monitoring) if the diurnal scaling factors are underestimated.

In the sixth and final step, we convert the satellite-derived instantaneous $PM_{2.5}$ to 24-h average $PM_{2.5}$ (our daily product) using $DSF_{i,x,y,h,model}$ as:

$$PM_{2.5,i,x,y,24-h,sat} = DSF_{i,x,y,h,model} \times PM_{2.5,i,x,y,h,sat} \quad (6)$$

We find that our daily (i.e., 24-h average) $PM_{2.5}$ product has spatial gaps due to the cloud cover and satellite-retrieval issues. This gap is filled when we average the daily $PM_{2.5}$ to generate the monthly and subsequently the annual $PM_{2.5}$ product. All the products are developed for the entire duration (26 February 2000–31 December 2019).

2.2. Comparison of Satellite-Derived and Ground-Based Daily and Annual $PM_{2.5}$

For cross-validation, we train our two-stage calibration model with 70% of the surface measurements randomly chosen from 120 CPCB sites. The remaining 30% of the data are used for validation. We find that the calibration improves the R^2 of satellite-derived instantaneous $PM_{2.5}$ and surface measurements during the overpass from 0.51 to 0.67. Since our main products are the daily (24-h average) and annual satellite-derived $PM_{2.5}$, we further compare these two against surface measurements from the CPCB network (Figure 3). Note that no further calibration is carried out after we estimate the daily $PM_{2.5}$ in the sixth and final step from the calibrated instantaneous $PM_{2.5}$. The slope (0.98) of the regression line and the intercept ($2.6 \mu\text{g}/\text{m}^3$) of the daily satellite-derived and surface measured $PM_{2.5}$ are close to the ideal values. The regression statistics are statistically significant at 95% CI following student's t -test ($p < 0.05$). Less than 0.5% of data points (out of the total number of samples = 34324) lie outside the 1:2 and 2:1 line. The cases ($<0.3\%$) where surface measurements are more than double the satellite-based $PM_{2.5}$ are confined to the Delhi NCR when the satellite fails to capture the extreme pollution events [13]. In the other cases ($<0.2\%$) where the surface measurements are much lower than the satellite-derived $PM_{2.5}$, the satellite data are overfitted. Most of the epidemiological studies [4] are carried out with annual $PM_{2.5}$ exposure and the NCAP also aims to reduce the annual $PM_{2.5}$ concentration. Our annual $PM_{2.5}$ product shows a RMSE of $7.2 \mu\text{g}/\text{m}^3$ and R^2 of 0.97 with the slope and the intercept similar to those of the daily product.

To understand the behavior of the error in the retrieved $PM_{2.5}$ dataset across a wide range of $PM_{2.5}$, we plot the retrieval bias (which is $PM_{2.5}$ from the CPCB sites— $PM_{2.5,sat}$) as a function of $PM_{2.5}$ from the CPCB sites (Figure 4). The median bias remains lower than $10 \mu\text{g}/\text{m}^3$ ($<5\%$) up to a $PM_{2.5}$ level of $200 \mu\text{g}/\text{m}^3$, beyond which the underestimation in $PM_{2.5,sat}$ starts to increase. Ground-based measurements reveal that 24-h $PM_{2.5}$ concentration in India usually remains below $200 \mu\text{g}/\text{m}^3$ in most of the days [28]. $PM_{2.5}$ concentration exceeds this range during the peak pollution season for a few days, that too, mostly in the Delhi NCR, which the satellite-derived data underestimate. Retrieval of these extreme cases is challenging in urban areas [13]. Further, we segregate the entire dataset of our daily product into various seasons (Figure A6) and various geographic regions (Figure A7) to understand if there is any systematic seasonal or regional bias in the dataset. Seasonally, we get the highest R^2 during the winter (DJF) season followed by the post-monsoon (ON) season with comparable RMSE, when the $PM_{2.5}$ level remains high (as shown in Section 3.2). In the other seasons, the RMSEs are lower and though R^2 values are slightly lower they are statistically significant ($p < 0.05$). We note that there are no ground-based monitoring sites in North and Northeast India. However, comparable regression statistics across the various geographical regions covering a diverse land use attest to the robustness and applicability of the dataset for air quality management. As the ground-based network

is being expanded including the rural areas under the NCAP, we expect further improvement in the product in future.

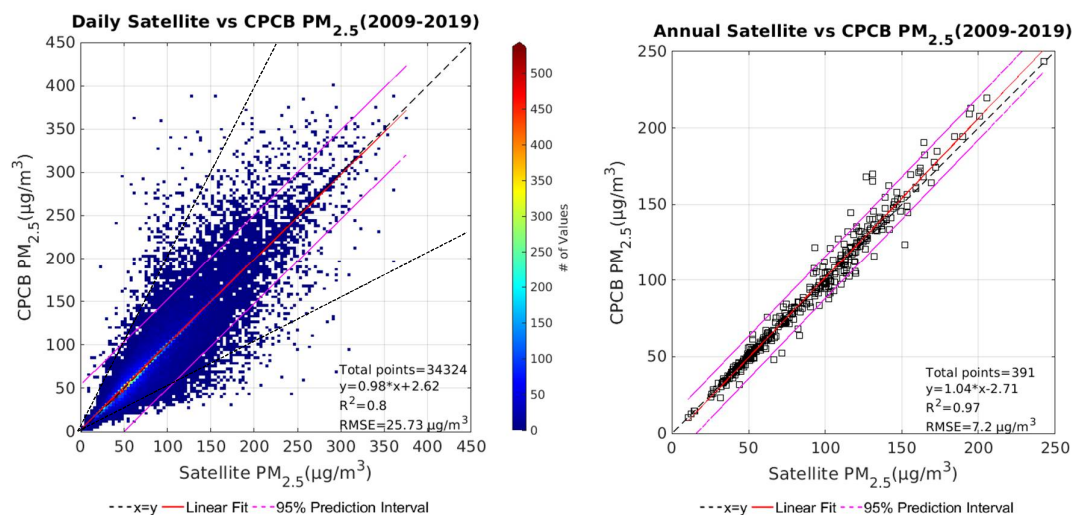


Figure 3. Regression statistics of (left) daily and (right) annual satellite-based and ground-based PM_{2.5} concentration over India. The points falling outside the 1:2 and 2:1 line (shown as dotted lines) are considered as the outliers (<0.5% for the daily PM_{2.5} product).

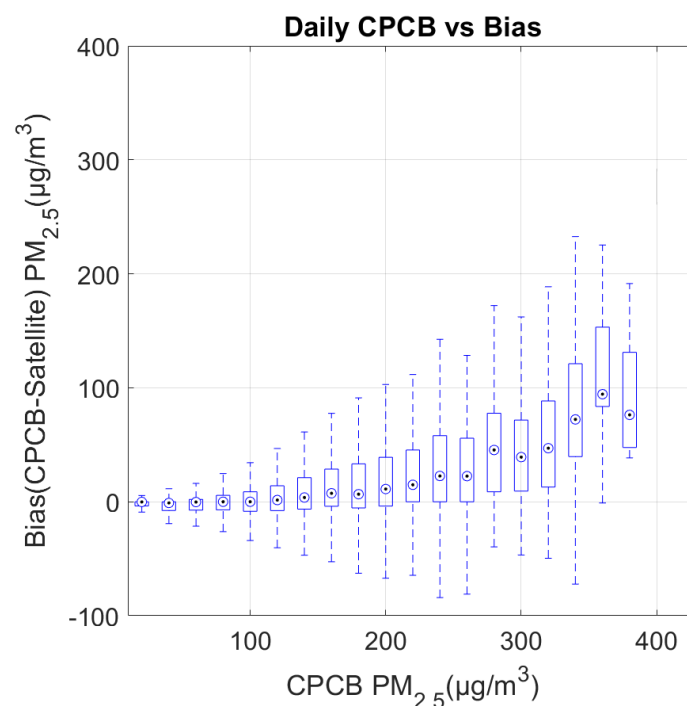


Figure 4. Variation in the bias in daily satellite-based PM_{2.5} concentrations relative to the ground-based measurements with an increase in the PM_{2.5} level. The box plots represent 5–95 percentile levels.

2.3. Analysis of PM_{2.5} Trends and Meteorological Parameters

We examine the PM_{2.5} trends in two different ways. First, we estimate the linear trends in annual PM_{2.5} within the last decade (2000 to 2009) and the present decade (2010 to 2019). Secondly, we estimate the mean seasonal PM_{2.5} over the entire duration for the winter (December–February), pre-monsoon (March–May), monsoon (June–September) and post-monsoon (October–November) seasons. The seasonal variations are examined in terms of the anomaly (i.e., mean seasonal PM_{2.5}–mean

annual $PM_{2.5}$) related to the annual concentration. The mean seasonal values are then used to estimate the linear trends in each season. The grids that are statistically significant ($p < 0.05$) following the student's t -test are marked.

We also analyze the planetary boundary layer (PBL) height and wind speed from the MERRA-2 reanalysis data. PBL height is inversely proportional to $PM_{2.5}$ as the particles get trapped if PBL height is low. Similarly, wind speed is also inversely proportional to $PM_{2.5}$ as stronger wind will allow particles to disperse easily. The combined effect of these two important meteorological factors on the $PM_{2.5}$ concentration is represented by the ventilation coefficient (VC), which is simply the product of PBL height and wind speed [29]. High VC implies a favorable condition for the dispersion, while low VC implies the condition as unfavorable. Therefore, the spatial and seasonal variations in $PM_{2.5}$ can be partially attributed to the changes in VC. We estimate the seasonal anomaly in VC with respect to the annual mean to understand the observed seasonal changes in $PM_{2.5}$ and the seasonal trends in VC to understand the seasonal trends.

2.4. Exposure Attribution

Population-weighted $PM_{2.5}$ exposure is estimated using the population data from the Indian Census. To separate the urban and rural $PM_{2.5}$, we analyze the Global Human Settlement Layer (GHSL) data [30]. This dataset was developed as part of a European Union project using 40-years of Landsat imagery that tracked the land use and land cover changes globally. Various other geospatial data (e.g., global cover of the artificial surface, open street maps, global urban extents and population distribution) are integrated with the land use data to identify each 1-km \times 1-km grid as one of the four classes—high-density urban (at least 1500 per km² population density), low-density urban (300–1500 per km² population density), rural (<300 per km² population density) and no-settlement (no permanent human occupancy). The GHSL provides the information in four distinct years—1975, 1990, 2000 and 2015. Here, we combine the high-density and low-density urban grids into a single urban class. Since the satellite-derived $PM_{2.5}$ is available from 26 February 2000, we consider the urban and rural $PM_{2.5}$ in 2001 as a baseline and estimate the changes in 2015. We assume that the human settlement pattern did not change much from 2000 to 2001 to affect our results.

The state/union territory (UT)-averaged urban and rural settlement fractions in India for the year 2000 and 2015 are shown in Figure A8. Overall, both the urban and rural settlement area has increased in India in a varying proportion to accommodate the growing population. We match each 1-km \times 1-km grid of satellite-based $PM_{2.5}$ with the GHSL data and estimate the urban and rural $PM_{2.5}$ population-weighted exposure in each state and UT for the years 2001 and 2015. We compare and report the statistics of rural and urban exposure along with the changes between 2001 and 2015 (Table A1). For the geographical locations of the states, UTs and the regions, see Figure A1.

3. Results

This section is divided into four subsections. First, we present the spatial pattern of $PM_{2.5}$ concentration over India in Section 3.1, followed by the seasonal changes in Section 3.2, the trend analysis in Section 3.3 and the urban–rural divide in $PM_{2.5}$ exposure in Section 3.4.

3.1. Spatial Pattern in $PM_{2.5}$ Concentration over India

The spatial distribution of $PM_{2.5}$ at the annual scale shown in Figure 5a mimics the spatial pattern observed by satellite-derived AOD (Figure 5b). Four points are notable in this figure. First, ambient $PM_{2.5}$ exceeds the annual NAAQS of 40 $\mu\text{g}/\text{m}^3$ in every state except the states of Jammu and Kashmir (including the new Ladakh UT), Himachal Pradesh, Sikkim, Arunachal Pradesh, Manipur and Nagaland (see Figure A2 for the geographical locations), where the population is sparse and a large part is covered by mountains. As of 2019, we find that 99.5% of the Indian districts (second administrative levels) do not meet the World Health Organization (WHO)-air quality guideline (AQG) of 10 $\mu\text{g}/\text{m}^3$. Second, the $PM_{2.5}$ level in the Indo-Gangetic Plain (IGP) and the western arid region is more than

double the annual NAAQS. The IGP is a low-lying fertile alluvial plain bounded by the Himalayas in the north and central Indian highlands in the south. Due to its fertility, it is densely populated with a population more than 700 million. Continuous emissions of primary $PM_{2.5}$ and secondary precursor gases (that contribute to $PM_{2.5}$ eventually) from a range of anthropogenic activities (e.g., household solid fuel use, power plants, industries, open biomass and solid-waste burning, vehicles, brick kilns, diesel generator sets, construction activities, etc.) coupled with unfavorable topography and meteorology lead to a massive $PM_{2.5}$ buildup. This $PM_{2.5}$ does not disperse away towards the north or south (bounded by the mountains); rather it oscillates east–west by the seasonal winds [31]. The only pathway of the pollution dispersion is through the Gangetic West Bengal towards the Bay of Bengal. The IGP, therefore, has become a giant valley trapped with high annual $PM_{2.5}$ that persists throughout the year. Third, the $PM_{2.5}$ shows a north (high)–south (low) gradient, which, to some extent, mimics the population distribution (and therefore the anthropogenic source distribution). The only exception is the western arid region, which is sparsely populated but highly polluted because of the large contribution of desert dust raised by wind [3]. Fourth, $PM_{2.5}$ is not proportionally (as compared to the IGP states) high over the states of Odisha, Telangana and Andhra Pradesh where AOD is high. In these regions, the condition for dispersion is favourable for February–October (as shown by low η values in Figure A4). We note that a large part of the IGP and many other states where the ambient $PM_{2.5}$ is high are rural. We discuss the urban–rural contrast in $PM_{2.5}$ exposure separately.

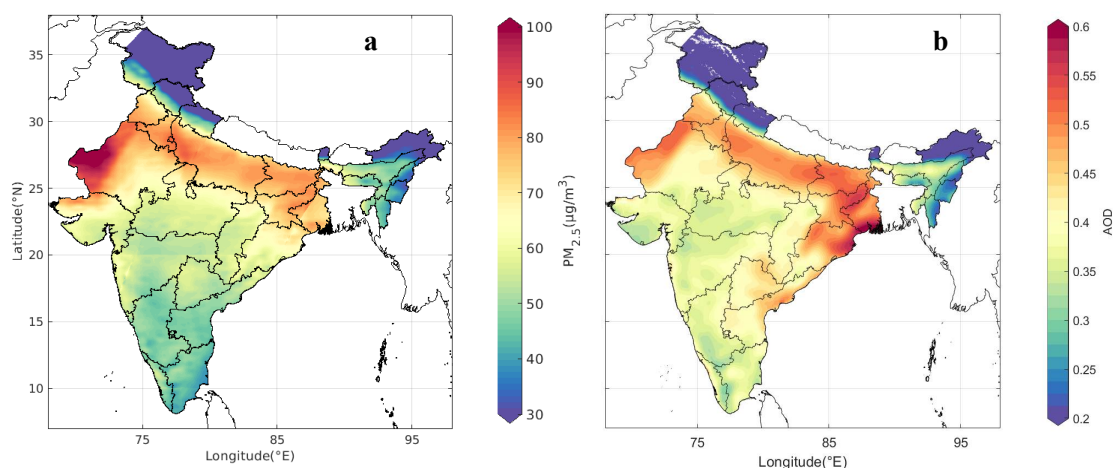


Figure 5. The spatial patterns of (a) annual $PM_{2.5}$ and (b) annual aerosol optical depth (AOD) averaged for the 20-year (2000–2019) period over India.

3.2. Seasonal Anomaly in $PM_{2.5}$ Concentration

Figure 6 shows the seasonal anomaly in $PM_{2.5}$ relative to the annual average $PM_{2.5}$ distribution. $PM_{2.5}$ is the highest in the winter season across the country except for the high-altitude regions in the north and the western arid region. This wintertime enhancement (a positive anomaly ranging from 5 to 40 $\mu g/m^3$ relative to the annual average) in $PM_{2.5}$ has been attributed to the additional emission from households (especially in the colder places due to space and water heating) and a stable atmosphere under calm conditions [12]. In the western arid region, dust activity remains at a minimum during the winter and in the high-altitude states of Jammu and Kashmir, Himachal Pradesh and Uttarakhand, major commercial activities remain closed due to extreme cold. Therefore, $PM_{2.5}$ shows a negative anomaly relative to the annual average. In the pre-monsoon season, the PBL expands with a rise in the surface temperature and wind speed increases, allowing $PM_{2.5}$ to be dispersed. As a result, $PM_{2.5}$ concentration decreases over the highly polluted IGP. However, this impact is partially compensated by the additional dust load in west India and emissions from seasonal open biomass burning over a large part of the northeast and peninsular India [3].

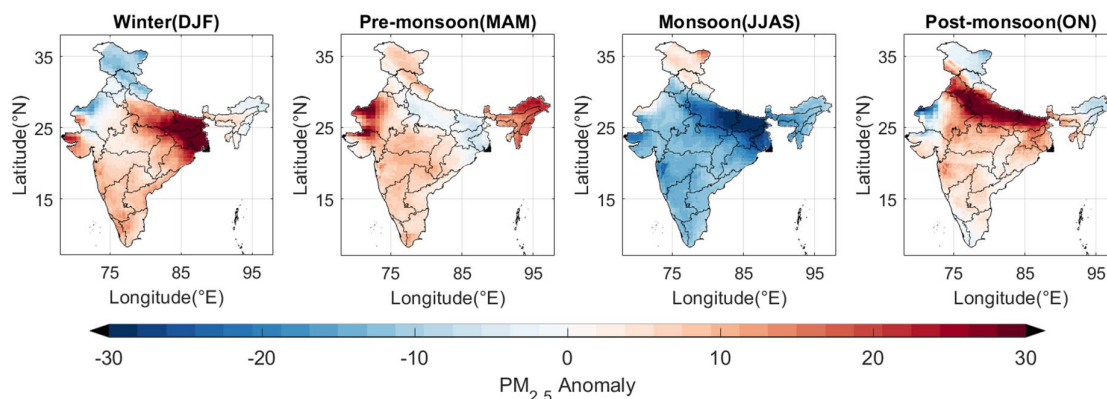


Figure 6. Spatial patterns of seasonal $PM_{2.5}$ anomaly (i.e., the difference between mean seasonal and mean annual $PM_{2.5}$) averaged over the 20-year (2000–2019) period over India.

$PM_{2.5}$ decreases in the monsoon season (as shown by a negative anomaly ranging from -5 to $-35 \mu\text{g}/\text{m}^3$ relative to the annual average) substantially as the particles are washed out by monsoon rain. The largest reduction is observed over the eastern IGP and along the west coast of India. In this season, $PM_{2.5}$ level remains lower than $40 \mu\text{g}/\text{m}^3$ over entire India except for the arid region in the west (where the monsoon rain is scanty) and the western IGP including Delhi NCR (where the emission strength is so high that the aerosol recovery overcompensates the loss due to washout [32]). However, we note that $PM_{2.5}$ does not meet the 24-h WHO–AQG ($25 \mu\text{g}/\text{m}^3$) on most of the days in most parts of the country even in this season, suggesting the severity of the problem. The temperature starts dropping with the monsoon retreat, especially in the north (including the IGP), northeast, west and central India in the post-monsoon season. In addition, the open biomass burning is prevalent across the country, more so in the western and central IGP, in this season, which adds to the regional $PM_{2.5}$ buildup due to a lower average PBL height [13].

3.3. Trends in $PM_{2.5}$ Concentration

We next present the rate of changes in annual $PM_{2.5}$ concentration (i.e., the annualized rate of changes) in the last and the current decade (top panel in Figure 7). The state-level statistics are shown in Table A1 (in the Appendix A). During the last decade, $PM_{2.5}$ over India shows a significant ($p < 0.05$) increase (by $>1 \mu\text{g}/\text{m}^3$ per year) over the states of Jharkhand, Chhattisgarh, Odisha, Telangana, Andhra Pradesh, Tamil Nadu, Kerala, and parts of Karnataka, Maharashtra and north-east India, while it decreases (not significantly though) over the high-altitude states of Jammu and Kashmir and Himachal Pradesh, and the Indian desert. In the current decade, the increase is found to be significant ($p < 0.05$) over the states of West Bengal, Odisha, Telangana, Maharashtra, and parts of Gujarat, Karnataka, Bihar, Uttar Pradesh, Madhya Pradesh and Uttarakhand. The decline continues over the eastern part of Jammu and Kashmir (now Ladakh UT) and parts of Rajasthan.

Emission data of primary $PM_{2.5}$, BC and OC and secondary gaseous precursors (e.g., SO_2 , NO_2 and volatile organics) from the Evaluating the Climate and Air Quality Impact of Short-lived Pollutants (ECLIPSE) emission inventory [33] suggest that the emissions from anthropogenic sources increased steadily over the last two decades everywhere in India with a larger increase in the eastern and central part of India dominated by mining activities and related industries and thermal power plants [34]. However, since we do not have continuous data, we can only qualitatively attribute the observed decadal trends in $PM_{2.5}$ to the rising emissions. The decadal changes in the VC (bottom panel in Figure 7) suggest that the meteorological condition became increasingly unfavorable in the last decade. This, coupled with the rising emissions, led to the observed increase in $PM_{2.5}$ in eastern and peninsular India. In the current decade, the VC does not show a significant trend. In fact, it has slightly increased (although not significantly) over western and central India, where we find a decrease in $PM_{2.5}$. However, in southeastern Maharashtra, the $PM_{2.5}$ increased despite an increase in VC. We only speculate that,

perhaps, the meteorological impact is overcompensated by the impact of rising emissions and regional transport in this region. For more quantitative interpretation, simulations from a chemical transport model are required and are beyond the scope of this work.

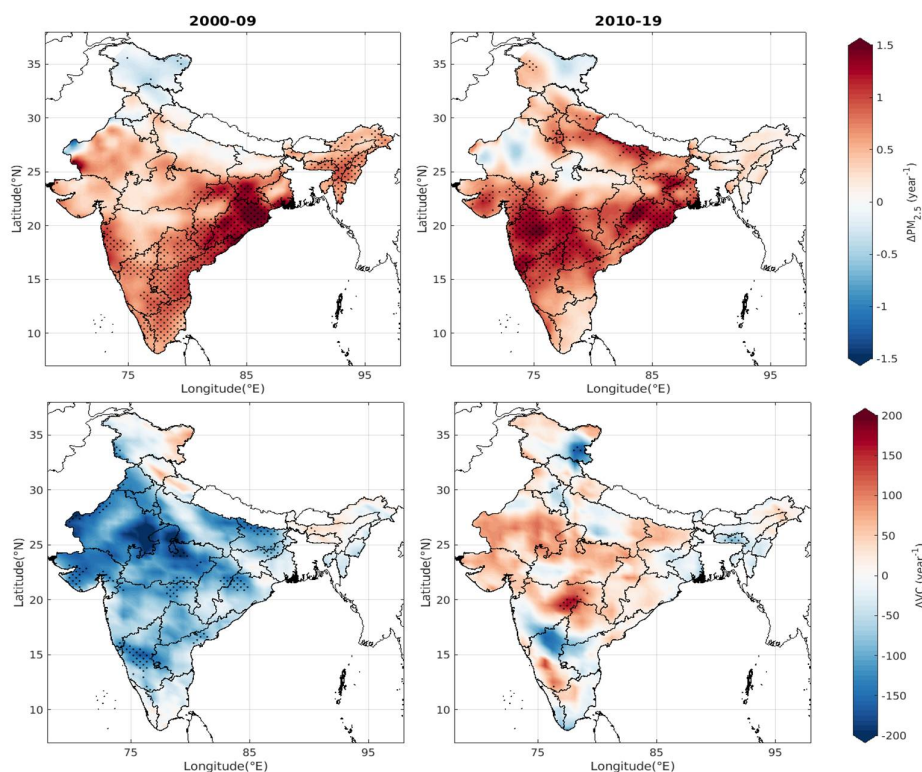


Figure 7. Spatial patterns of the annualized rate of changes in (top panel) $PM_{2.5}$ (in $\mu g/m^3$ per year) and (bottom panel) ventilation coefficient, VC (in m^2/s per year) over India during the last decade (2000–2009) and the current decade (2010–2019). The statistically significant trends ($p < 0.05$) are identified as stippled marks.

The annualized rate of changes at the seasonal scale is displayed in Figure 8. We note several key features. First, ambient $PM_{2.5}$ shows a significant increase ($p < 0.05$) over almost the entire country in the post-monsoon and winter seasons, except over the arid regions in the west and high-altitude regions in the north and northeast. The largest trends ($>2 \mu g/m^3$ per year) are observed over the IGP, eastern and southeast India (along the east coast), large parts of peninsular India and the state of Gujarat. In the pre-monsoon season, $PM_{2.5}$ increases over east, northeast and peninsular India, which are affected by open biomass burning [35]. The decreasing trend over west and northwest India is perhaps attributed to the declining dust activity [36]. In the monsoon season when $PM_{2.5}$ generally remains low (Figure 6), no apparent trend is observed, except over some patches in the west and central IGP. In terms of major emission sources, open biomass burning is a seasonal source and is observed in the pre-monsoon (after the wheat cultivation) and the post-monsoon (after the rice cultivation) seasons. Studies have suggested that the post-monsoon burning has increased post-2009 in the states of Punjab and Haryana [13] while the pre-monsoon burning marginally increased all over the country [37]. Since the $PM_{2.5}$ shows an increasing trend over the peninsular and east India in the three seasons, the largest trend in annual $PM_{2.5}$ is observed in these regions (Figure 9a). The trend over the IGP, the most polluted region in India (and one of the top polluted regions in the world), is governed mainly by the rising $PM_{2.5}$ during the post-monsoon to winter seasons. Overall, the trends are higher over eastern and peninsular India ($>1.6\%$ per year) where the number of hazy days has been increasing at a faster rate than over the IGP [38] where the annual $PM_{2.5}$ is the highest but the rate of increase is $<1.2\%$ per year (Figure 9b).

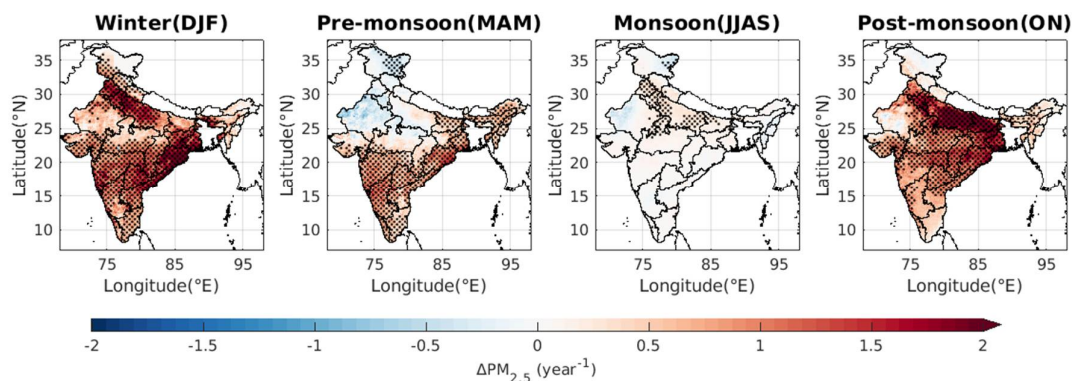


Figure 8. Spatial patterns of the annualized rate of changes in seasonal $PM_{2.5}$ (in $\mu g/m^3$ per year) over India during the last 20 years. The statistically significant trends ($p < 0.05$) are identified as stippled marks.

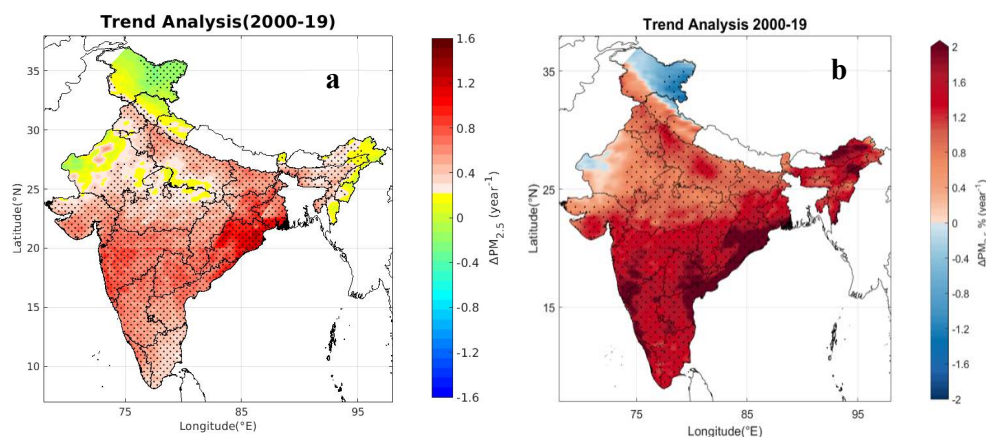


Figure 9. Spatial patterns of (a) the annualized rate of changes in $PM_{2.5}$ (in $\mu g/m^3$ per year) and (b) the relative changes (in % per year) over India during the 20 years. The statistically significant trends ($p < 0.05$) are identified as stippled marks.

3.4. Urban vs. Rural $PM_{2.5}$

Unlike the developed countries where $PM_{2.5}$ is considered to be an urban problem, we observe that high $PM_{2.5}$ cuts across the urban–rural transect. We therefore present comparative statistics of urban vs. rural population-weighted $PM_{2.5}$ exposure in Figure 10 for the year 2001 and the state-averaged changes in urban and rural population-weighted exposure from 2001 to 2015 in Figure 11. We observe that the urban $PM_{2.5}$ exposure in Delhi increased by 10.9% from 82.2 (5–95 percentile ranges: 27.8–168.9) $\mu g/m^3$ in 2001 to 91.3 (33.7–190.7) $\mu g/m^3$ in 2015. During the same period, the rural $PM_{2.5}$ exposure increased by 11.9% from 81.1 (27.8–163.4) $\mu g/m^3$ to 90.7 (32.5–192.5) $\mu g/m^3$. We point out that though the urban and rural exposure is comparable, the urban area (80%) is disproportionately higher in Delhi than the rural area (10%). The remaining 10% area does not have any permanent human settlement and therefore can be considered as the background. Several key features are now presented. First, population-weighted $PM_{2.5}$ exposure increased in all the states/UTs from 2001 to 2015 (Table A1). Second, in 2001, all the states/UTs except Arunachal Pradesh (28.1 $\mu g/m^3$), Manipur (38.9 $\mu g/m^3$), Mizoram (39.7 $\mu g/m^3$), Nagaland (35.2 $\mu g/m^3$) and Puducherry (24.6 $\mu g/m^3$) had rural $PM_{2.5}$ exposure exceeding the NAAQS. In 2015, the rural $PM_{2.5}$ exposure remained below the NAAQS only in Arunachal Pradesh (33.5 $\mu g/m^3$), Puducherry (26.9 $\mu g/m^3$) and Sikkim (39.7 $\mu g/m^3$). Sikkim was the only state where rural exposure reduced. Third, in 2001, the urban $PM_{2.5}$ exposure exceeded the NAAQS in all the states/UTs except Arunachal Pradesh (34.1 $\mu g/m^3$), Daman and Diu (36.2 $\mu g/m^3$), Goa (33.9 $\mu g/m^3$),

Kerala ($36.7 \mu\text{g}/\text{m}^3$), Nagaland ($37.4 \mu\text{g}/\text{m}^3$), Puducherry ($25.3 \mu\text{g}/\text{m}^3$) and Tamil Nadu ($38.0 \mu\text{g}/\text{m}^3$), while in 2015, it remained below the NAAQS only in two states/UTs—Arunachal Pradesh ($38.7 \mu\text{g}/\text{m}^3$) and Puducherry ($30.3 \mu\text{g}/\text{m}^3$). Fourth, both rural and urban $\text{PM}_{2.5}$ exposure exceeded the double of the NAAQS in 2001 in only Delhi (81.0 and $82.3 \mu\text{g}/\text{m}^3$), while in 2015, it happened in five states—Delhi (90.7 and $91.3 \mu\text{g}/\text{m}^3$), Haryana (84.5 and $85.7 \mu\text{g}/\text{m}^3$), Uttar Pradesh (82.4 and $82.8 \mu\text{g}/\text{m}^3$), Bihar (81.3 and $81.4 \mu\text{g}/\text{m}^3$) and Jharkhand (81.1 and $83.2 \mu\text{g}/\text{m}^3$). Finally, in most of the states, the urban and rural $\text{PM}_{2.5}$ exposure are comparable.

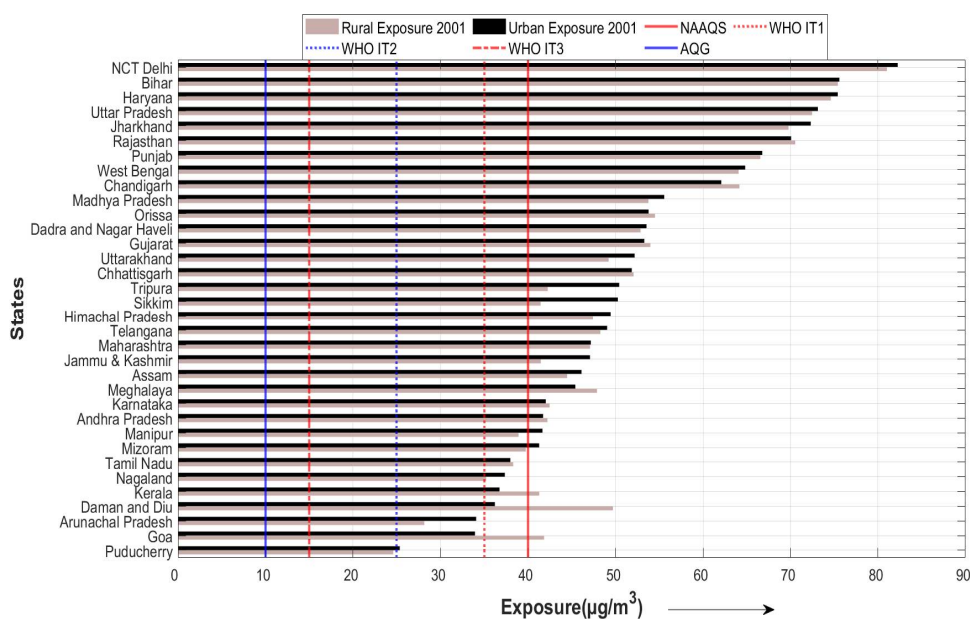


Figure 10. State-wise urban and rural population-weighted $\text{PM}_{2.5}$ exposure in 2001. World Health Organization air quality guideline, WHO AQG ($10 \mu\text{g}/\text{m}^3$) and the interim targets (IT-1: $35 \mu\text{g}/\text{m}^3$; IT-2: $25 \mu\text{g}/\text{m}^3$ and IT-3: $15 \mu\text{g}/\text{m}^3$), and national ambient air quality standard, NAAQS ($40 \mu\text{g}/\text{m}^3$) are marked by the vertical lines. The states/union territories are arranged in the decreasing order of $\text{PM}_{2.5}$ level.

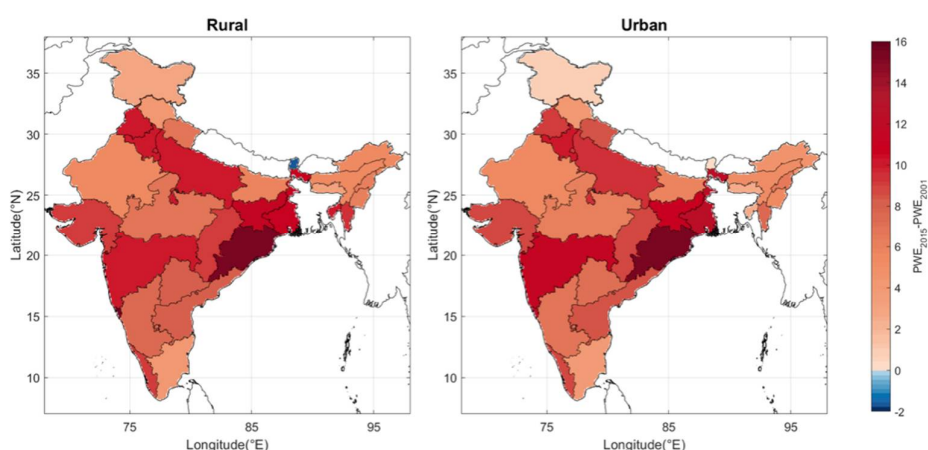


Figure 11. Changes (in $\mu\text{g}/\text{m}^3$) in (left) rural and (right) urban population-weighted $\text{PM}_{2.5}$ exposure in 2015 relative to 2001 (shown in Figure 9).

4. Discussion

In this work, we develop and present a 20-year ambient $\text{PM}_{2.5}$ database for India at a high (1-km) spatial resolution. The data are disseminated freely through a web portal ‘satellite-based application of

air quality monitoring and management at a national scale', SAANS (www.saans.co.in) for use in air quality management, epidemiological studies and creating awareness amongst the citizens, especially from the states/UTs where the ground-based measurements are unavailable or scanty. Our work adds to the recent efforts of retrieving $PM_{2.5}$ at high resolution [19,22] for an improved exposure assessment. We note the following issues for the proper interpretation of our database. First, we could not calibrate the scaling factor with ground-based data before 2009 and assume the calibration factors would be the same in this period. Second, the evaluation of the data is restricted to the urban centres as rural air quality monitoring from the surface does not exist in India. In future, when the surface network will be expanded to the rural area, the true error in satellite-based $PM_{2.5}$ can be identified. We discuss several important implications and potential applications of our database.

High $PM_{2.5}$ in the rural area is not surprising as a large fraction of the population still relies on solid fuel for domestic use (cooking, heating and lighting) [4]. These emissions do not remain confined with the household and filtrate out to pollute ambient air. Household sources are found to be the largest contributor to ambient $PM_{2.5}$ in India [39–42]. This implies that poor air quality in India is not an urban-centric problem; rather it is a regional scale problem. Therefore, India requires a regional scale management strategy that transcends urban boundaries and focuses on regional airsheds. The NCAP focuses on 122 non-attainment cities. Many cities/towns in India do not have any ground-based measurements and hence whether they are non-attainment could not be determined during the early phase of the NCAP. Using our database, we found that 436 cities/towns with a population more than 100,000 (as per the 2011 Indian Census) exceed the NAAQS in 2019. We recommend setting up ground-based monitoring in these cities/towns on a priority basis.

The Government of India launched a program—Pradhan Mantri Ujjwala Yojana (PMUY, the Prime Minister's program of clean household fuel)—in 2014 to empower rural women by promoting clean cooking fuel (LPG) in the rural areas. This policy is highly important as mitigating emissions completely from the household sources can potentially help India achieve the NAAQS [43]. As the PMUY is rolled out, it lacks a mechanism to track its progress. Since the household sources contribute more than 50% to ambient $PM_{2.5}$ in the rural areas [44], successful implementation of PMUY with sustained usage should arrest or even reverse the increasing trend in rural $PM_{2.5}$ in recent years.

The high-resolution database will enable track the local hotspots within a city, especially where a single or no ground-based monitoring sites exist. It also will facilitate identification of the representative sites for the expansion of the CPCB network under the NCAP in the coming years.

In India, the epidemiological studies are either time-series (as summarized in [12]) or by design establishing the association, not causality [45], or the acute exposure impact on health outcomes like birthweight [46]. For the chronic exposure impacts on mortality and various health outcomes, we still rely on the GBD framework [1,2,4] that does not include any cohort study from India on ambient $PM_{2.5}$ exposure. Our database will be highly useful to fill this important gap by planning retrospective cohorts with the existing health data and generating India-specific exposure-response functions.

5. Conclusions

Using a novel high-resolution (1-km) ambient $PM_{2.5}$ database, we examine the trends in $PM_{2.5}$ concentrations in India over two decades (2000–2019). Our key conclusions are: (1) the urban and rural ambient $PM_{2.5}$ exposure increased by an almost similar margin from 2001 to 2015; (2) particulate air quality in India is a regional scale problem and needs a coordinated clean air action plan addressing the urban and rural sources simultaneously; and (3) mitigating emissions during October–February in the north and east India and December–May in peninsular India would arrest the rising annual $PM_{2.5}$ trend.

Author Contributions: Conceptualization, S.D.; methodology, S.D. and B.P.; software, B.P. and K.D.; validation, S.D., B.P., P.B. and K.D.; formal analysis, B.P.; investigation, S.D. and B.P.; resources, S.D.; data curation, P.B., K.B., A.K., F.I., P.G. and V.K.S.; writing—original draft preparation, S.D.; writing—review and editing, S.D., B.P., P.B., K.D., K.B., A.K., F.I., S.C., D.G., P.G., V.K.S.; visualization, B.P.; supervision, S.D.; project administration,

S.D. and D.G.; funding acquisition, S.D. and D.G. All authors have read and agreed to the published version of the manuscript.

Funding: This research was funded by the Central Pollution Control Board, India under the National Clean Air Program.

Acknowledgments: MAIAC AOD data are available from the Langley Research Centre Data Archive and the MERRA-2 reanalysis data are available from the NASA Goddard Earth Science Data Information Service Centre. GHSL data are freely available from the project website (<https://ghsl.jrc.ec.europa.eu/data.php>). The authors acknowledge Nitu and Koseqa for help in data compilation. S.D. acknowledges the support for the Institute Chair position by Indian Institute of Technology Delhi. The Department of Science and Technology (Govt. of India)—Funds for Improvement of Science and Technology Infrastructure in universities and higher educational institutions (DST-FIST) grant (SR/FST/ES-II-016/2014) is acknowledged for the computing support at IIT Delhi. We thank the anonymous reviewers for providing feedback that helped improve the original manuscript.

Conflicts of Interest: P.G. and V.K.S. are employees of the Central Pollution Control Board, which funded this research under the National Clean Air Program. They contributed intellectually to this study. All other authors declare no conflict of interest.

Appendix A

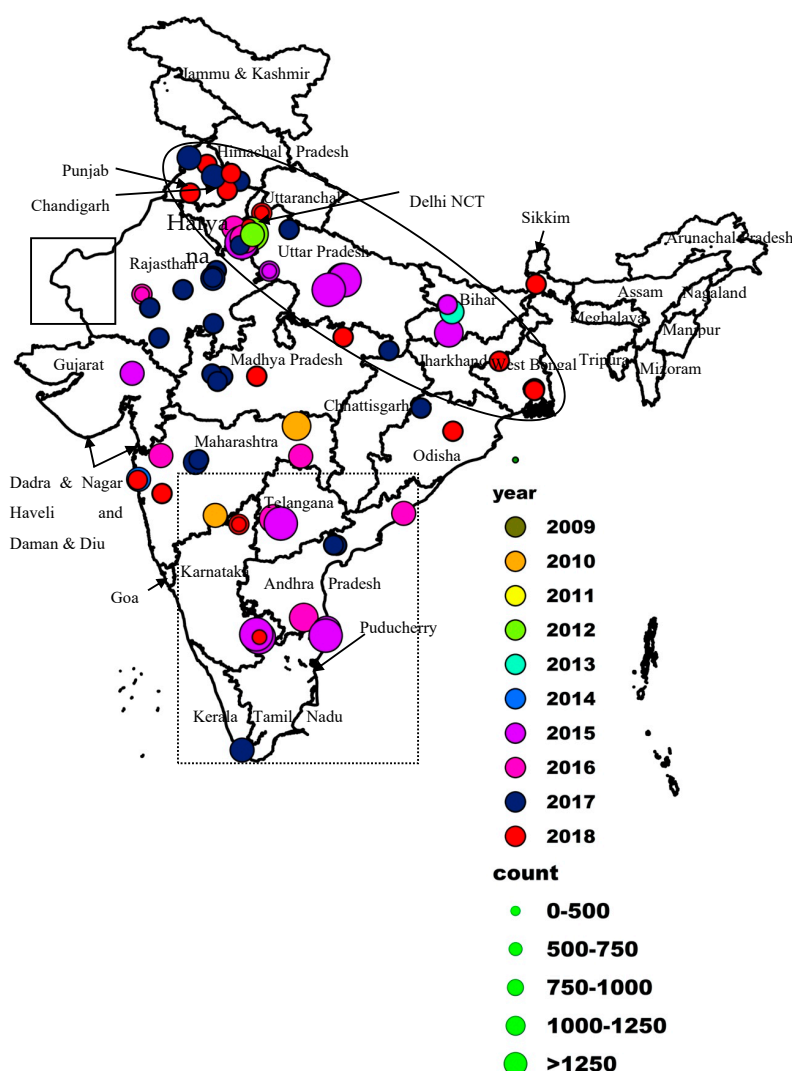


Figure A1. Central Pollution Control Board monitoring sites that are used to calibrate the satellite-PM_{2.5} dataset. The location of the Indo-Gangetic Plain, IGP (as discussed in the main text) is demarcated by oval shape, the Thar Desert by the rectangular box and Peninsular India by a dotted box. The size of the circles indicates the number of data and the colors represent the year from which the measurements started in each site.

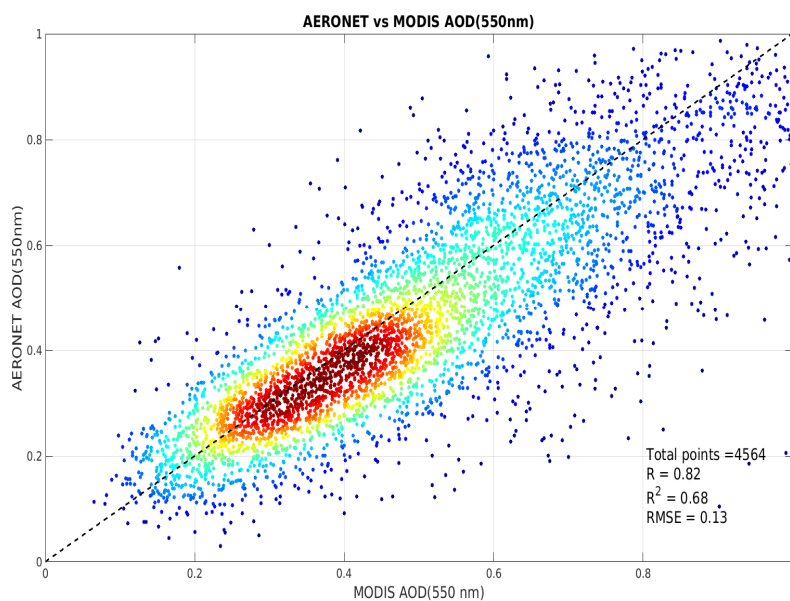


Figure A2. Comparison between Moderate Resolution Imaging Spectroradiometer–Multiangle Implementation of Atmospheric Correction (MODIS–MAIAC) AOD and Aerosol Robotic Network (AERONET) AOD over India. Three AERONET sites with multi-year data are chosen for the analysis—Kanpur (26.5° N, 80.3° E), Gandhi College (25.9° N, 84.1° E) and Jaipur (26.9° N and 75.8° E). Kanpur, Gandhi College and Jaipur sites have been operating since 2001, 2006 and 2009, respectively.

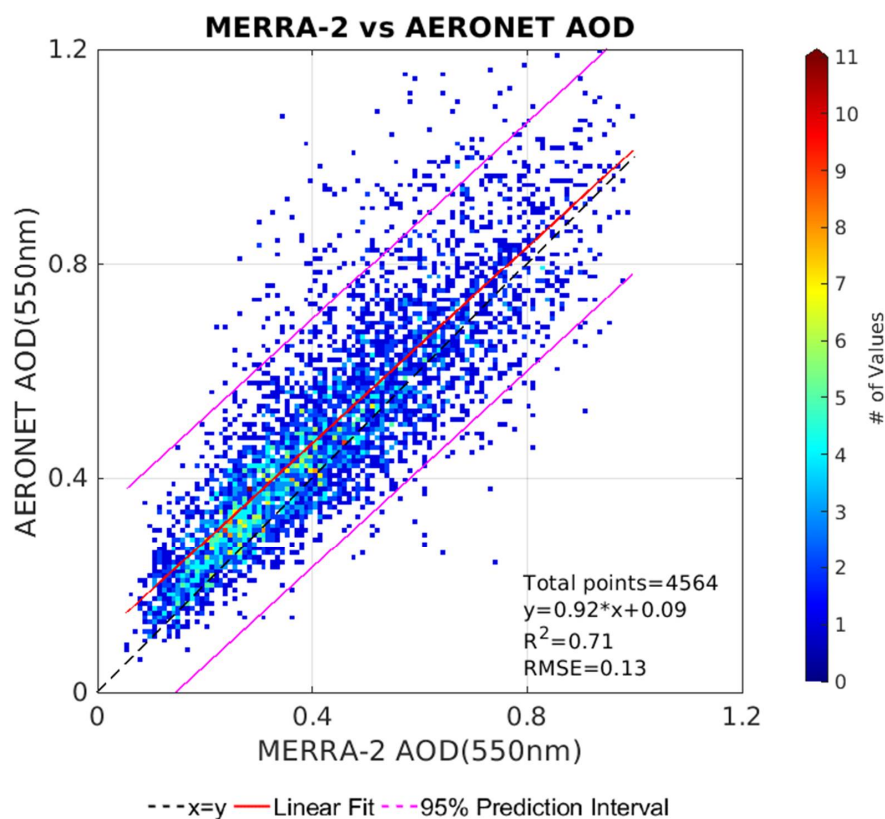


Figure A3. Correlation between hourly Modern-Era Retrospective analysis for Research and Applications Version 2 (MERRA-2) and AERONET AOD in India along with the regression statistics.

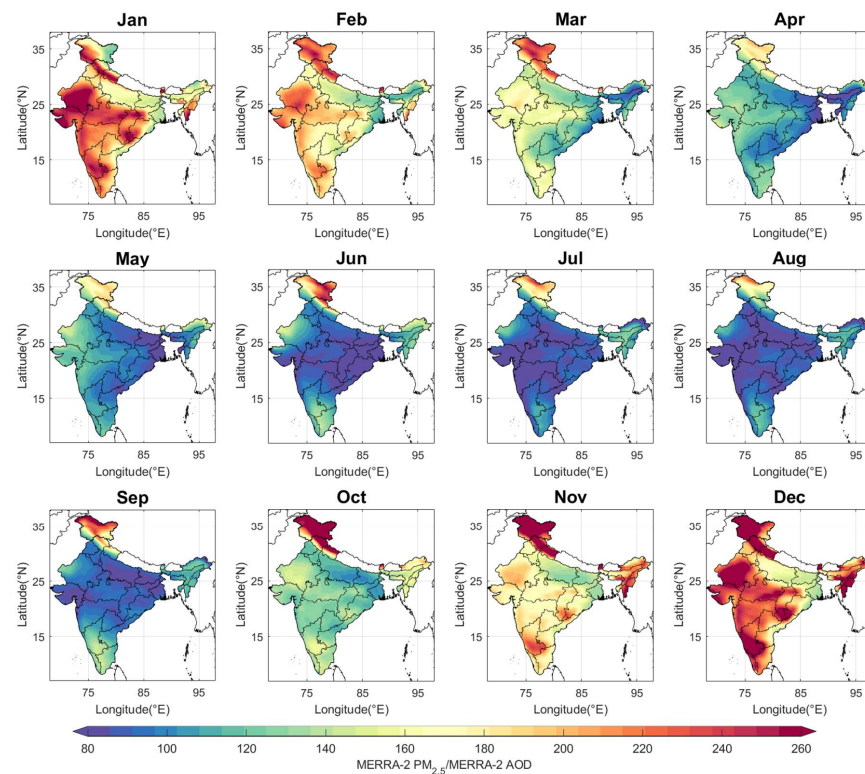


Figure A4. Spatial patterns of mean monthly η over India as derived from MERRA-2 data. η values are derived for each day during the entire study period and used to estimate PM_{2.5} from satellite AOD.

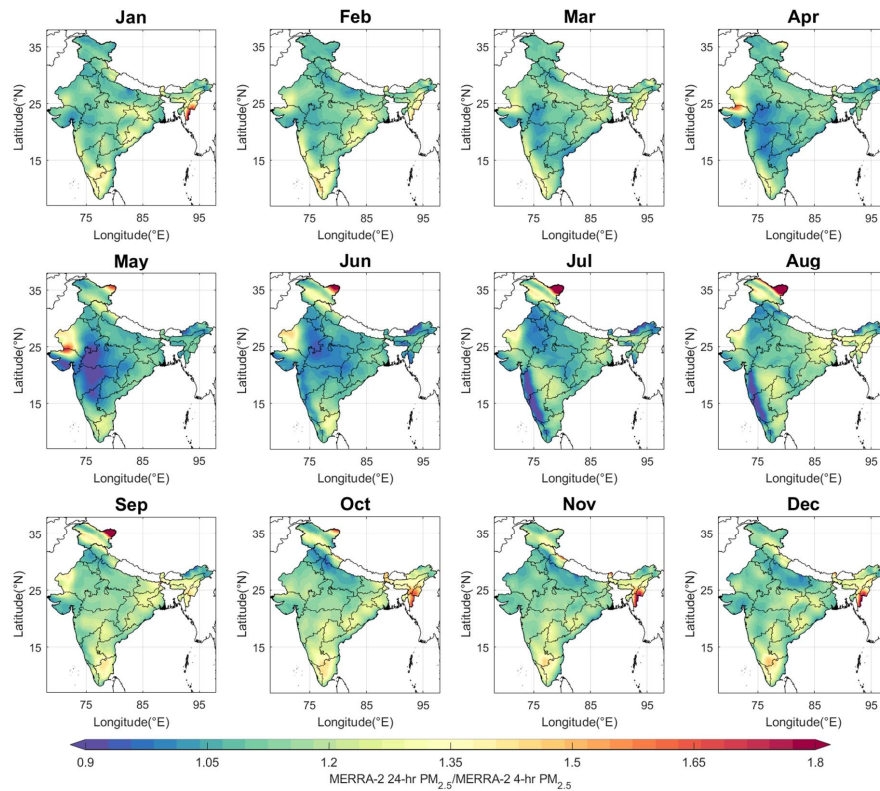


Figure A5. Spatial patterns of mean monthly diurnal scaling factor over India derived from MERRA-2 data. The diurnal scaling factor values are derived for each day during the entire study period and used to estimate 24-h PM_{2.5} from instantaneous (i.e., during the satellite-overpass time) PM_{2.5}.

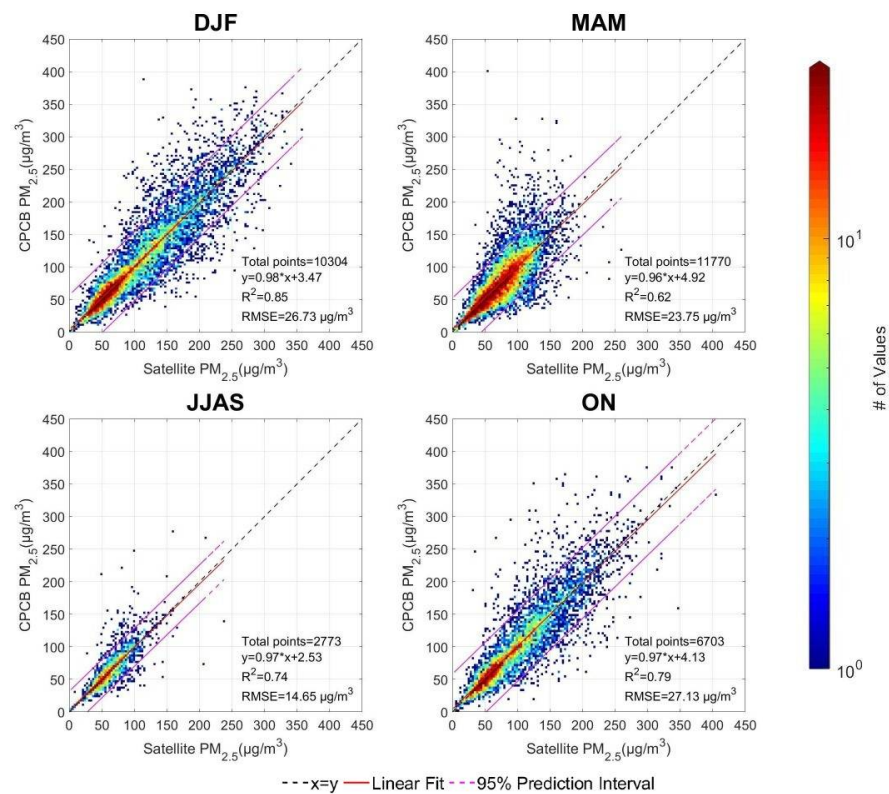


Figure A6. Regression statistics of the satellite-based daily $PM_{2.5}$ with measurements from Central Pollution Control Board (CPCB) sites for the winter (DJF), pre-monsoon (MAM), monsoon (JJAS) and post-monsoon (ON) seasons over India.

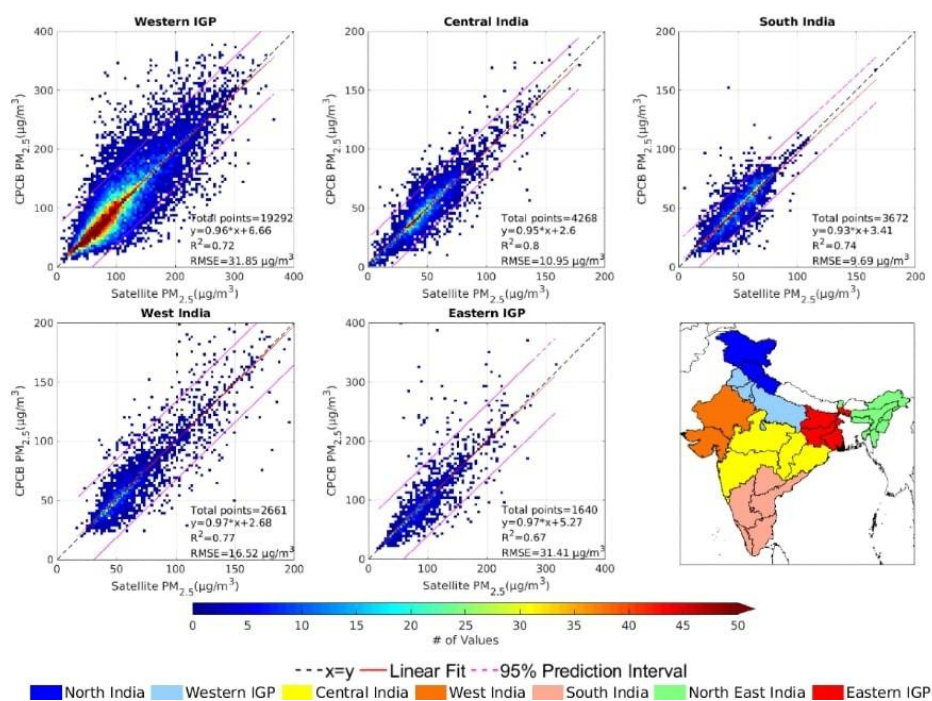


Figure A7. Regression statistics of the satellite-based daily $PM_{2.5}$ with measurements from CPCB sites for the various geographic regions (shown in the bottom right panel) over India. There are no ground-based monitoring sites in Northeast and North India to validate the retrieved $PM_{2.5}$.

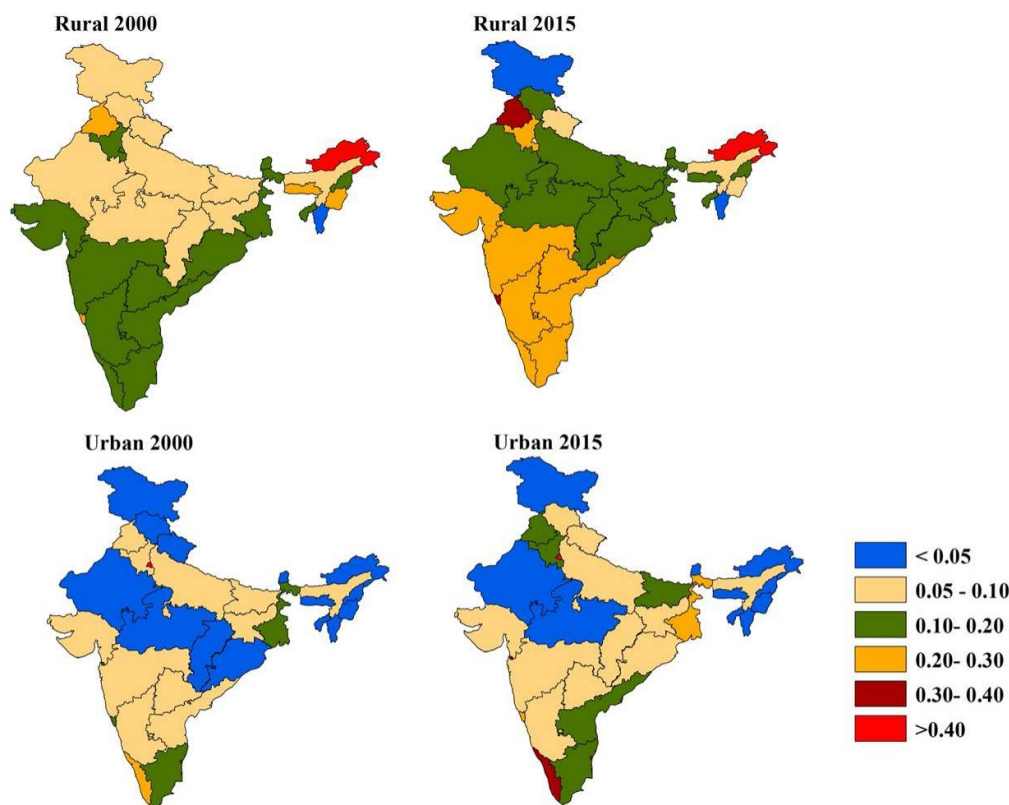


Figure A8. State-averaged fractional area (e.g., <0.05 means <5% area) populated by the urban and rural settlements in India in 2000 and 2015. Note that the remaining area has no permanent human settlement.

Table A1. State/UT level statistics of population-weighted PM_{2.5} exposure along with 5–95 percentile ranges for the years 2001 and 2019. The states/UTs are arranged in the decreasing order of urban area fraction in 2015. The urban and rural exposure changes shown here are estimated for the period 2001 to 2015, since the Global Human Settlement Layer (GHSL) data are available up to 2015.

State/UT	PM _{2.5} in 2001 ($\mu\text{g}/\text{m}^3$)	PM _{2.5} in 2019 ($\mu\text{g}/\text{m}^3$)	Change in Urban Exposure from 2001–2015 (%)	Change in Rural Exposure from 2001–2015 (%)
Chandigarh	62.0 (23.9–127.2)	61.9 (24.5–141.5)	18.7	13.4
Delhi national capital territory	82.3 (27.9–169.8)	86.7 (34.2–185.3)	10.9	11.9
Puducherry	34.6 (22.4–56.7)	44.9 (21.1–80.5)	19.7	9.5
Dadra and Nagar Haveli	53.3 (24.2–99.9)	62.9 (24.6–121.9)	19.0	20.3
Kerala	40.5 (19.6–75.4)	51.1 (20.4–105.1)	24.2	21.9
West Bengal	66.6 (27.3–156.8)	78.2 (29.4–166.4)	19.3	17.2
Goa	44.1 (18.5–86.4)	60.4 (19.7–120.3)	36.4	37.3
Daman and Diu	54.6 (25.9–95.8)	61.2 (26.2–114.7)	25.7	17.3
Bihar	76.2 (27.6–175.9)	80.2 (29.7–176.2)	7.6	7.8
Punjab	70.3 (31.4–140)	73.4 (31.7–140.8)	13.6	14.9
Tamil Nadu	38.5 (20.5–69.8)	47.2 (21.9–91.6)	10.1	11.1
Haryana	75.9 (29.9–155.1)	81.5 (33.5–162.4)	13.6	13.2
Andhra Pradesh	42.3 (21.1–77.8)	54.6 (21.9–121.2)	20.1	18.9
Uttar Pradesh	71.8 (26.3–163.8)	79.3 (31–164.7)	13.2	13.7
Telangana	47.5 (23.6–89.1)	58.4 (24.1–113.7)	14.6	16.5
Jharkhand	68.4 (27.4–144.9)	79.1 (28.1–164.5)	15.1	16.2
Karnataka	42.4 (16.9–84.3)	51.3 (16.8–104.5)	16.6	17.1
Gujarat	54.7 (31.2–92.9)	63.4 (28–108.3)	16.5	16.7
Maharashtra	48.3 (21.7–83)	58.1 (22.4–107)	24.0	21.0
Assam	45.7 (16.4–111.5)	48.4 (17.3–97.9)	11.0	12.7
Odisha	55.7 (26.1–109.2)	72.7 (25.6–153.1)	28.2	28.3
Tripura	50.1 (17–149.7)	48.6 (16.8–102.1)	4.9	23.8
Uttarakhand	42.5 (12.4–68.3)	41.4 (15.4–73.8)	16	13.7

Table A1. Cont.

State/UT	PM _{2.5} in 2001 ($\mu\text{g}/\text{m}^3$)	PM _{2.5} in 2019 ($\mu\text{g}/\text{m}^3$)	Change in Urban Exposure from 2001–2015 (%)	Change in Rural Exposure from 2001–2015 (%)
Madhya Pradesh	53.8 (24.6–106.2)	60.3 (26.4–117)	11.2	12.8
Chhattisgarh	51.8 (23.7–96.3)	60.2 (23.2–121.5)	17.3	17.6
Himachal Pradesh	27.0 (13.3–52.8)	23.9 (12.1–50.2)	8.0	8.5
Rajasthan	74.8 (35.4–139.4)	74.7 (35.8–133)	7.5	7.9
Manipur	35.6 (5.6–94.9)	36.1 (6.5–90.2)	13.4	16.2
Jammu and Kashmir	17.1 (9.8–38.7)	13.1 (6.5–33.5)	2.1	7.3
Nagaland	36.2 (7.2–95.2)	37.9 (7.7–96.6)	17.5	17.1
Meghalaya	49.6 (16.5–139.7)	49.9 (17.4–107.4)	5.4	6.4
Mizoram	41.0 (7.5–115.3)	42.3 (8.3–97.7)	18.2	24.1
Arunachal Pradesh	23.3 (4.1–63)	25.9 (4.9–77.9)	13.4	18.9
Sikkim	27.9 (5.1–59.2)	29.4 (6.1–55)	0.2	−4.3

References

- Dandona, L.; Dandona, R.; Kumar, G.A.; Shukla, D.K.; Paul, V.K.; Balakrishnan, K.; Prabhakaran, D.; Tandon, N.; Salvi, S.; Dash, A.P.; et al. Nations within a nation: Variations in epidemiological transition across the states of India, 1990–2016 in the Global Burden of Disease Study. *Lancet* **2017**, *390*, 2437–2460. [\[CrossRef\]](#)
- Cohen, A.J.; Brauer, M.; Burnett, R.; Anderson, H.R.; Frostad, J.; Estep, K.; Balakrishnan, K.; Brunekreef, B.; Dandona, L.; Dandona, R.; et al. Estimates and 25-year trends of the global burden of disease attributable to ambient air pollution: An analysis of data from the Global Burden of Disease Study 2015. *Lancet* **2017**, *389*, 1907–1918. [\[CrossRef\]](#)
- Dey, S.; Di Girolamo, L.; van Donkelaar, A.; Tripathi, S.N.; Gupta, T.; Mohan, M. Decadal exposure to fine particulate matter (PM_{2.5}) in the Indian Subcontinent using remote sensing data. *Remote Sens. Environ.* **2012**, *127*, 153–161. [\[CrossRef\]](#)
- Balakrishnan, K.; Dey, S.; Gupta, T.; Dhaliwal, R.S.; Brauer, M.; Cohen, A.J.; Stanaway, J.D.; Beig, G.; Joshi, T.K.; Aggarwal, A.N.; et al. The impact of air pollution on deaths, disease burden, and life expectancy across the states of India: The Global Burden of Disease Study 2017. *Lancet Planet. Health* **2019**, *3*, 26–39. [\[CrossRef\]](#)
- Chowdhury, S.; Dey, S. Cause-specific premature death from ambient PM_{2.5} exposure in India: Estimate adjusted for baseline mortality. *Environ. Int.* **2016**, *91*, 283–290. [\[CrossRef\]](#) [\[PubMed\]](#)
- Apte, J.; Brauer, M.; Cohen, A.J.; Ezzati, M.; Pope, C.A. Ambient PM_{2.5} reduces global and regional life expectancy. *Environ. Sci. Technol. Lett.* **2018**, *5*, 546–551. [\[CrossRef\]](#)
- Martin, R.V.; Brauer, M.; van Donkelaar, A.; Shaddick, G.; Narain, U.; Dey, S. no one knows which city has the highest concentration fine particulate matter. *Atmos. Environ.* **2019**, *3*, 100040. [\[CrossRef\]](#)
- Pant, P.; Lal, R.M.; Guttikunda, S.K.; Russell, A.G.; Nagpure, A.S.; Ramaswami, A.; Peltier, R.E. Monitoring particulate matter in India: Recent trends and future outlook. *Air Qual. Atmos. Health* **2019**, *12*, 45–58. [\[CrossRef\]](#)
- Brauer, M.; Guttikunda, S.K.; Nishad, K.A.; Dey, S.; Tripathi, S.N.; Weagle, C.; Martin, R.V. Examination of monitoring approaches for ambient air pollution: A case study for India. *Atmos. Environ.* **2019**, *216*, 116940. [\[CrossRef\]](#)
- Gordon, T.; Balakrishnan, K.; Dey, S.; Rajagopalan, S.; Thornburg, J.; Thurston, G.; Agrawal, A.; Collman, G.; Guleria, R.; Limaye, S.; et al. Air pollution health research priorities for India: Perspectives of the Indo-U.S. communities of researchers. *Environ. Int.* **2018**, *119*, 100–108. [\[CrossRef\]](#)
- Pal, R.; Chowdhury, S.; Dey, S.; Sharma, A.R. 18-year ambient PM_{2.5} exposure and nightlight trends in Indian cities: Vulnerability assessment. *Aerosol Air Qual. Res.* **2018**, *18*, 2332–2342. [\[CrossRef\]](#)
- Pande, P.; Dey, S.; Chowdhury, S.; Choudhary, P.; Ghosh, S.; Srivastava, P.; Sengupta, B. Seasonal transition in PM₁₀ exposure and associated all-cause mortality risks in India. *Environ. Sci. Technol.* **2018**, *52*, 8756–8763. [\[CrossRef\]](#) [\[PubMed\]](#)
- Chowdhury, S.; Dey, S.; Di Girolamo, L.; Smith, K.R.; Pillarisetti, A.; Lyapustin, A. Tracking ambient PM_{2.5} buildup in Delhi national capital region during the dry season over 15 years using a high-resolution (1-km) satellite aerosol dataset. *Atmos. Environ.* **2019**, *204*, 142–150. [\[CrossRef\]](#)

14. Mhawish, A.; Banerjee, T.; Sorek-Hamer, M.; Bilal, M.; Lyapustin, A.; Chatfield, R.; Broday, D.M. Estimation of high-resolution PM_{2.5} over the Indo-Gangetic Plain by fusion of satellite data, meteorology, and land use variables. *Environ. Sci. Technol.* **2020**, *54*, 7891–7900. [CrossRef]
15. Yazdi, M.D.; Kuang, Z.; Dimakopouou, K.; Baratt, B.; Suel, E.; Amini, H.; Lyapustin, A.; Katsouyanni, K.; Schwartz, J. Predicting fine particulate matter (PM_{2.5}) in the Greater London area: An ensemble approach using machine learning methods. *Remote Sens.* **2020**, *12*, 914. [CrossRef]
16. van Donkelaar, A.; Martin, R.V.; Brauer, M.; Kahn, R.A.; Levy, R.C.; Verduzco, C.; Villeneuve, P.J. Global estimates of ambient particulate matter concentrations from satellite-based aerosol optical depth: Development and application. *Environ. Health Perspect.* **2010**, *118*, 847–855. [CrossRef] [PubMed]
17. van Donkelaar, A.; Martin, R.V.; Brauer, M.; Hsu, N.C.; Kahn, R.A.; Levy, R.C.; Lyapustin, A.; Sayer, A.M.; Winker, D.M. Global estimates of fine particulate matter using a combined geophysical-statistical method with information from satellites, models, and monitors. *Environ. Sci. Technol.* **2016**, *50*, 3762–3772. [CrossRef]
18. van Donkelaar, A.; Martin, R.V.; Brauer, M.; Boys, B.L. Use of satellite observations for long-term exposure assessment of global concentrations of fine particulate matter. *Environ. Health Perspect.* **2015**, *123*, 135–143. [CrossRef]
19. Hammar, M.S.; van Donkelaar, A.; Li, C.; Lyapustin, A.; Sayer, A.M.; Hsu, N.C.; Levy, R.C.; Garay, M.J.; Kalashnikova, O.V.; Kahn, R.A.; et al. Global estimates and long-term trends of fine particulate matter concentrations (1998–2018). *Environ. Sci. Technol.* **2020**, *54*, 7879–7890. [CrossRef]
20. Shaddick, G.; Thomas, M.L.; Amini, H.; Broday, D.; Cohen, A.; Frostad, J.; Green, A.; Gummy, S.; Liu, Y.; Martin, R.V.; et al. Data integration for the assessment of population exposure to ambient air pollution for global burden of disease assessment. *Environ. Sci. Technol.* **2018**, *52*, 9069–9078. [CrossRef]
21. Lyapustin, A.; Wang, Y.; Korkin, S.; Huang, D. MODIS collection 6 MAIAC algorithm. *Atmos. Meas. Tech.* **2018**, *11*, 5741–5765. [CrossRef]
22. Mhawish, A.; Banerjee, T.; Sorek-Hamer, M.; Lyapustin, A.; Broday, D.M.; Chatfield, R. Comparison and evaluation of MODIS Multi-angle Implementation of Atmospheric Correction (MAIAC) aerosol product over South Asia. *Remote Sens. Environ.* **2019**, *224*, 12–28. [CrossRef]
23. Holben, B.; Eck, T.; Slutsker, I.; Tanré, D.; Buis, J.; Setzer, A.; Vermote, E.; Reagan, J.; Kaufman, Y.; Nakajima, T.; et al. AERONET—A federated instrument network and data archive for aerosol characterization. *Remote Sens. Environ.* **1998**, *66*, 1–16. [CrossRef]
24. Kloog, I.; Chudnovsky, A.A.; Just, A.C.; Nordio, F.; Koutrakis, P.; Coull, B.A.; Lyapustin, A.; Wang, Y.; Schwartz, J. A new hybrid spatio-temporal model for estimating daily multi-year PM_{2.5} concentrations across northeastern USA using high resolution aerosol optical depth data. *Atmos. Environ.* **2014**, *95*, 581–590. [CrossRef]
25. Buchard, V.; Randles, C.A.; Da Silva, A.M.; Darmenov, A.; Colarco, P.R.; Govindaraju, R.; Ferrare, R.; Hair, J.; Beyersdorf, A.J.; Ziemba, L.D.; et al. The MERRA-2 aerosol reanalysis, 1980-onward, Part II: Evaluation and case studies. *J. Clim.* **2017**, *30*, 6851–6872. [CrossRef]
26. Ram, K.; Sarin, M.M.; Tripathi, S.N. Temporal trends in atmospheric PM_{2.5}, PM₁₀, elemental carbon, organic carbon, water-soluble organic carbon, and optical properties: Impact of biomass burning emissions in the Indo-Gangetic Plain. *Environ. Sci. Technol.* **2010**, *46*, 686–695. [CrossRef]
27. Navinya, C.D.; Vinoj, V.; Pandey, S.K. Evaluation of PM_{2.5} surface concentrations simulated by NASA's MERRA Version 2 aerosol reanalysis over India and its relation to air quality index. *Aerosol Air Qual. Res.* **2020**, *20*, 1329–1339. [CrossRef]
28. Central Pollution Control Board, Government of India Website. Available online: www.cpcb.nic.in (accessed on 1 May 2020).
29. Gani, S.; Bhandari, S.; Seraj, S.; Wang, D.S.; Patel, K.; Soni, P.; Arub, Z.; Habib, G.; Ruiz, L.H.; Apte, J.S. Submicron aerosol composition in the world's most polluted megacity: The Delhi aerosol supersite study. *Atmos. Chem. Phys.* **2019**, *19*, 6843–6859. [CrossRef]
30. Dijkstra, L.; Poelmann, H. A harmonized definition of cities and rural areas: The new degree of urbanization. *Eur. Comm. Urban Reg. Pol.* **2014**. Available online: https://ec.europa.eu/regional_policy/sources/docgener/work/2014_01_new_urban.pdf (accessed on 1 May 2020).
31. Dey, S.; Di Girolamo, L. A climatology of aerosol optical and microphysical properties over the Indian Subcontinent from 9 years (2000–2008) of Multiangle Imaging SpectroRadiometer (MISR) data. *J. Geophys. Res.* **2010**, *115*, D15204. [CrossRef]

32. Chowdhury, S.; Dey, S.; Ghosh, S.; Saud, T. Satellite-based estimates of aerosol washout and recovery over India during monsoon. *Aerosol Air Qual. Res.* **2016**, *16*, 629–639. [\[CrossRef\]](#)
33. Stohl, A.; Aamaas, B.; Amann, M.; Baker, L.H.; Bellouin, N.; Bernsten, T.K.; Boucher, O.; Cherian, R.; Collins, W.; Daskalakis, N.; et al. Evaluating the climate and air quality impacts of short-lived pollutants. *Atmos. Chem. Phys.* **2015**, *15*, 10529–10566. [\[CrossRef\]](#)
34. Upadhyay, A.; Dey, S.; Goyal, P.; Dash, S.K. Projection of near-future anthropogenic PM_{2.5} over India using statistical approach. *Atmos. Environ.* **2018**, *186*, 178–188. [\[CrossRef\]](#)
35. Bikkina, S.; Andersson, A.; Kirillova, E.N.; Holmstrand, H.; Tiwari, S.; Srivastava, A.K.; Bisht, D.S.; Gustafsson, O. Air quality in megacity Delhi affected by countryside biomass burning. *Nat. Sustain.* **2019**, *2*, 200–205. [\[CrossRef\]](#)
36. Pandey, S.K.; Vinoj, V.; Landu, K.; Babu, S.S. Declining pre-monsoon dust loading over South Asia: Signature of a changing regional climate. *Sci. Rep.* **2017**, *7*, 16062. [\[CrossRef\]](#) [\[PubMed\]](#)
37. Sahu, L.K.; Sheel, V.; Pandey, K.; Yadav, R.; Saxena, P.; Gunthe, S. Regional biomass burning trends in India: Analysis of satellite fire data. *J. Earth Sys. Sci.* **2015**, *124*, 1377–1387. [\[CrossRef\]](#)
38. Thomas, A.; Sarangi, C.; Kanawade, V.P. Recent increase in winter hazy days over Central India and the Arabian Sea. *Sci. Rep.* **2019**, *9*, 17409. [\[CrossRef\]](#)
39. Chafe, Z.; Brauer, M.; Klimont, Z.; van Dingenen, R.; Mehta, S.; Rao, S.; Riah, K.; Dentener, F.; Smith, K.R. Household cooking with solid fuels contributes to ambient PM_{2.5} air pollution and the burden of disease. *Environ. Health Perspect.* **2014**, *122*, 1314–1320. [\[CrossRef\]](#)
40. Lelieveld, J.; Evans, J.S.; Fnais, M.; Giannadaki, D.; Pozzer, A. The contribution of outdoor air pollution sources to premature mortality on a global scale. *Nature* **2015**, *525*, 367–371. [\[CrossRef\]](#)
41. Conibear, L.; Butt, E.W.; Knote, C.; Arnold, S.R.; Spracklen, D.V. residential energy use emissions dominate health impacts from exposure to ambient particulate matter in India. *Nat. Commun.* **2018**, *9*, 1–9. [\[CrossRef\]](#)
42. GBD MAPS Working Group 2018. Burden of disease attributable to major air pollution sources in India. Health Effects Institute, Boston, MA, USA. *Spec. Rep.* **2018**, *21*. Available online: <https://www.healtheffects.org/publication/gbd-air-pollution-india> (accessed on 1 May 2020).
43. Chowdhury, S.; Dey, S.; Guttikunda, S.; Pillarisetti, A.; Smith, K.R.; Di Girolamo, L. Indian ambient air quality standard is achievable by completely mitigating emissions from household sources. *Proc. Natl. Acad. Sci. USA* **2019**, *116*, 10711–10716. [\[CrossRef\]](#) [\[PubMed\]](#)
44. Upadhyay, U.; Dey, S.; Chowdhury, S.; Goyal, P. Expected health benefits from mitigation of emissions from major anthropogenic PM_{2.5} sources in India: Statistics at state level. *Environ. Pollut.* **2018**, *242*, 1817–1826. [\[CrossRef\]](#) [\[PubMed\]](#)
45. Spears, D.; Dey, S.; Chowdhury, S.; Scovronick, N.; Vyas, S.; Apte, J. The association of early-life exposure to ambient PM_{2.5} and later-childhood age-for-height in India: An observational study. *Environ. Health* **2019**, *18*, 62. [\[CrossRef\]](#) [\[PubMed\]](#)
46. Balakrishnan, K.; Ghosh, S.; Thangavel, G.; Sambandam, S.; Mukhopadhyay, K.; Puttaswamy, N.; Sadasivam, A.; Ramaswamy, P.; Johnson, P.; Kuppuswamy, R.; et al. Exposure to fine particulate matter (PM_{2.5}) and birthweight in a rural-urban, mother-child cohort in Tamil Nadu, India. *Environ. Res.* **2018**, *161*, 524–531. [\[CrossRef\]](#)

Publisher’s Note: MDPI stays neutral with regard to jurisdictional claims in published maps and institutional affiliations.



© 2020 by the authors. Licensee MDPI, Basel, Switzerland. This article is an open access article distributed under the terms and conditions of the Creative Commons Attribution (CC BY) license (<http://creativecommons.org/licenses/by/4.0/>).